ACS chemical biology

LETTERS

pubs.acs.org/acschemicalbiology

A Luminescent Biosensor with Increased Dynamic Range for Intracellular cAMP

Brock F. Binkowski,* Braeden L. Butler, Peter F. Stecha, Christopher T. Eggers, Paul Otto, Kris Zimmerman, Gediminas Vidugiris, Monika G. Wood, Lance P. Encell, Frank Fan, and Keith V. Wood

Promega Corporation, 2800 Woods Hollow Rd., Madison, Wisconsin 53711, United States

Supporting Information

ABSTRACT: The second messenger cAMP is a key mediator of signal transduction following activation of G-protein coupled receptors. Investigations on Gs-coupled receptors would benefit from a second messenger assay that allows continuous monitoring of kinetic changes in cAMP concentration over a broad dynamic range. To accomplish this, we have evolved a luminescent biosensor for cAMP to better encompass the physiological concentration ranges present in living cells. When compared to an immunoassay, the evolved biosensor construct was able to accurately track both the magnitude and kinetics of cAMP change using a far less labor intensive format. We demonstrate the utility of this construct to detect a broad range of receptor activity, together with showing suitability for use in high-throughput screening.

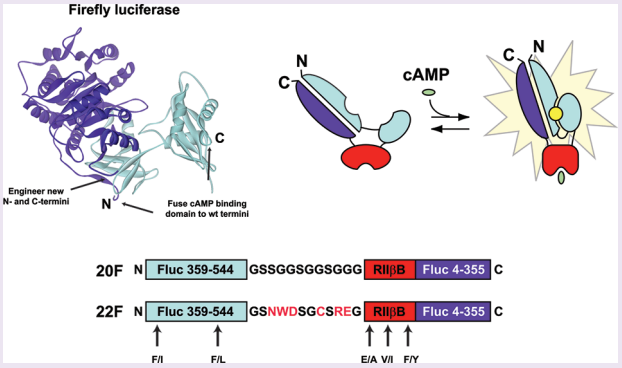

Cyclic adenosine monophosphate (cAMP) in mammalian cells is a key second messenger of signal transduction mediated by G-protein coupled receptors (GPCRs). By regulating the activity of downstream effectors such as protein kinase A (PKA), the intracellular concentration of cAMP plays a vital role in cellular metabolism and is broadly relevant to pharmacological mechanisms. In recent years, insight has been gained on the molecular mechanisms underlying the temporal control of cAMP signaling, where cAMP levels have been shown to rise and fall rapidly within the cell following receptor activation and response desensitization.[1−3] Traditional assays for cAMP using antibody detection or radiolabeled precursors are cumbersome for monitoring temporal changes since a separate population of cells are processed for each time point.[4] In response to this limitation, genetically encoded FRET or BRET biosensors have been created by combining cAMP-binding domains with fluorescent or luminescent proteins.[4,5] Although these have been valuable in revealing spatial and temporal dynamics of intracellular cAMP signaling, limitations in dynamic range may hinder their ability to accurately portray the full physiological range of intracellular cAMP.[4,5]

Limitations in dynamic range can lead to significant artifacts for an intracellular biosensor. A highly sensitive biosensor may be prone to saturation at elevated levels of cAMP, while conversely, having a higher detection range to minimize saturation may limit sensitivity.[4,5] From our own experience, saturation effects can lead to misrepresentations of compound pharmacology, such as reduced apparent potency or efficacy for agonists of Gs-coupled receptors. In lytic assays, operation within a linear range can be assured by increasing cell numbers or diluting samples into the corresponding range of a standard curve. Because this is not easily achieved with a biosensor and few comparisons to lytic assays have been reported,[6] uncertainty can exist regarding the reliability of biosensor measurements. Broad linearity coupled with high sensitivity is needed to consistently represent the range of intracellular cAMP concentrations present within living cells. Moreover, given the importance of GPCRs in drug discovery, it is desirable for such biosensors to be amendable for high-throughput screening (HTS).

We have increased the dynamic range of a novel biosensor design that couples a cAMP-binding domain from PKA (RIIβB) to a circularly permuted form of *Photinus pyralis* luciferase.[7] Our initial construct, 20F, showed large increases in light output following activation of endogenous Gs-coupled receptors in HEK293 cells, where it appeared to represent real-time changes in the concentration of intracellular cAMP [7] in the cytosol.[8] Although able to detect small changes in basal cAMP levels with good sensitivity (Supplementary Figure 1),[9] 20F appears to approach saturation in living cells under certain experimental conditions. Moreover, the maximal response of 20F was diminished in non-HEK293 cell types (Supplementary Figure 2).

To overcome these limitations, we evolved the 20F construct *via* introduction of five amino acid changes in the N-terminal luciferase fragment and cAMP binding domain, together with six amino acid changes in the N-terminal linker peptide. The resultant construct, 22F, exhibits a substantially increased linear

Received: July 18, 2011
Accepted: September 19, 2011
Published: September 20, 2011

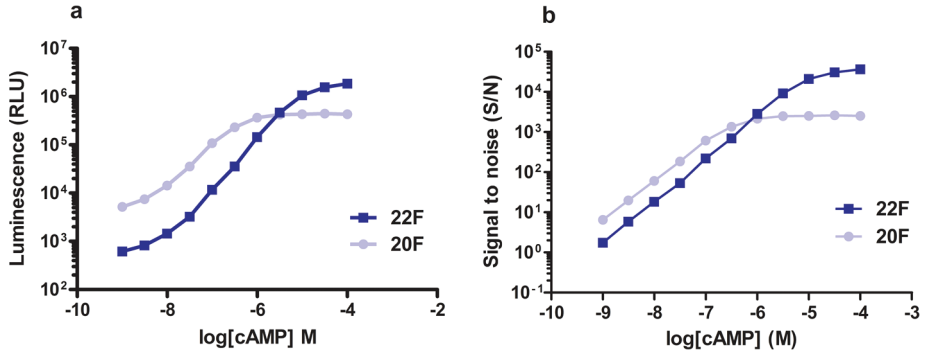

Figure 1. Increased dynamic range of the 22F construct *in vitro*. (a) Rabbit reticulocyte lysate expressing 22F or 20F was incubated with varying concentrations of cAMP for 15 min, and aliquots were combined with luciferase assay reagent for luminescence measurement. (b) Signal-to-noise determination at each concentration tested. S/N = (RLU conc. X − RLU, vehicle)/(standard deviation, vehicle).

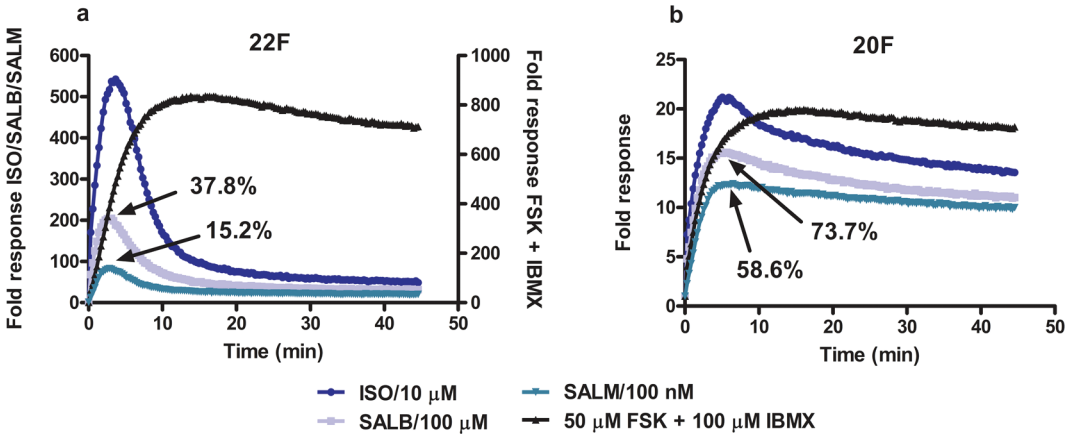

Figure 2. Increased dynamic range of the 22F construct in living cells. Transient expression of the (a) 22F construct or (b) 20F construct in HEK293 cells followed by treatment with saturating concentrations of ADRB2 full or partial agonists at 28 °C. Fold response was calculated as the luminescence of a given well receiving compound divided by the basal luminescence of the same well prior to compound addition. Using the maximal response for each, percent efficacy values are indicated for the partial agonists relative to the maximal response elicited by saturating ISO. ISO, isoproterenol; SALB, salbutamol; SALM, salmeterol; FSK, forskolin; IBMX, 3-isobutyl-1-methylxanthine. n = 1 per trace.

detection range. Based on *in vitro* detection of cAMP, the maximal S/B of 22F was increased 35-fold (100- *vs* 3500-fold at saturation) together with a 30-fold increase in EC_{50} (0.3 to 9 μM) (Figure 1, panel a). The composite effect of these changes increases the linear range by 30-fold at higher concentrations of cAMP, to 0.003−10 μM for 22F relative to 0.001−0.3 μM for 20F (Figure 1, panel b), while leaving ligand selectivity unaltered (Supplementary Figure 3). The linear range of 22F *in vitro* overlaps the reported dynamic range of several FRET/BRET based constructs, and the overall dynamic range of 22F (0.003−100 μM) encompasses the composite dynamic range of all FRET/BRET based biosensors.[5] Although the sensitivity (S/N) of 22F is reduced up to 4-fold relative to that of 20F at concentrations less than 1 μM, the detection limit is substantially lower than the detection limits reported for FRET/BRET based sensors.[5]

The increased linear range of 22F substantially enhances its ability to reveal both the magnitude and dynamics of receptor signaling in living cells. For example, 22F is better able to discriminate between the efficacy of full or partial agonists of the endogenous ADRB2 receptor in HEK293 cells compared to 20F (Figure 2, Supplementary Figures 4 and 5). In these experiments, the signaling dynamics from 20F tended to more closely follow the response produced by forskolin plus phosphodiesterase (PDE) inhibitor (Figure 2, panel b), suggesting the biosensor response may be approaching saturation. In contrast, the response of 22F to the agonists was well below the level produced with forskolin plus PDE inhibitor (Figure 2, panel a). Moreover, the respective agonists elicited notably different response levels with 22F with markedly different response dynamics. Relieving the apparent constraint of saturation greatly increased the overall response window, where 22F showed an 800-fold response range versus only 20-fold for 20F. Greatly increased response dynamics were also evident for 22F in other cell types (Supplementary Figure 2).

The accuracy of 22F for representing the true signaling dynamics within cells can be assessed through comparisons to a lytic assay of cAMP. For this purpose, we used a highly sensitive immunoassay (EIA) with a detection range of 0.078−20 nM, where this level of sensitivity is required owing to cAMP dilution upon cell lysis. Upon serial treatment of cells with agonists, antagonists, and forskolin, both assays showed strikingly similar response profiles in both signal magnitude and kinetics (Figure 3, panel a). When treated with isoproterenol alone, a close correlation was again seen between 22F and EIA, with response dynamics similar to those in previous work using a FRET based sensor.[1] Importantly, a far weaker correlation was seen with 20F

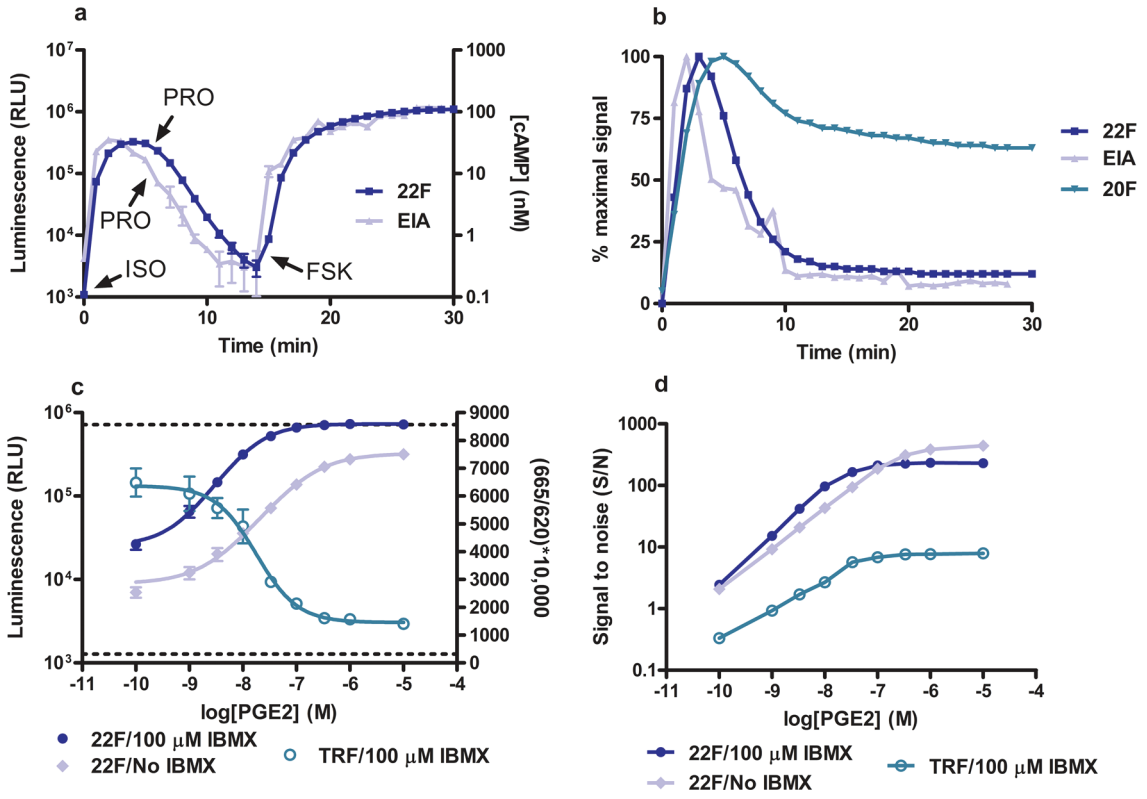

Figure 3. Comparison of the 22F construct to two separate immunoassays. (a, b) HEK293 cells transiently expressing the 22F construct were split for either luminescence measurements or EIA. (a) Cells treated sequentially with 1 μM ISO (ADRB2 agonist), 10 μM PRO (ADRB2 antagonist), and 10 μM FSK at the indicated time points at 28 °C. (b) Cells treated with 100 nM ISO alone at 28 °C, where HEK293 cells expressing the 20F construct alone were included for comparison. (c, d) Comparison to an antibody-based assay utilizing TRF in 384-well format. Cells transiently expressing the 22F construct were split for either luminescence measurements or TRF, where the cell number was chosen to optimize the response for TRF. (c) Cells treated with varying concentrations of PGE2 agonist for 30 min. For TRF, the raw data was plotted as the emission ratio [(665 nm)/(620 nm) × 10,000]. Dotted lines represent the upper and lower asymptotes of the four parameter logistic curve fit of the cAMP standard curve for TRF. XC50 values: 148.1 nM, 22F no IBMX; 14.3 nM, 22F 100 μM IBMX; 17.8 nM, TRF 100 μM IBMX. Z′ values at 10 μM PGE2: 0.78, 22F no IBMX; 0.82, 22F 100 μM IBMX; 0.56, TRF 100 μM IBMX (d) Signal-to-noise determination at each concentration tested. S/N = (RLU conc. X − RLU, vehicle)/(standard deviation, vehicle). Four parameter logistic curve fits using GraphPad Prism 4. ISO, isoproterenol; PRO, propranolol; FSK, forskolin. Error bars represent standard deviation.

in both experiments (Figure 3, panel b, Supplementary Figure 6), and samples greater than 20 nM required dilution for EIA to remain in the linear portion of the standard curve.

To demonstrate the suitability of 22F for HTS, we compared the performance to a commonly used lytic assay based on time-resolved fluorescence (TRF) in low volume 384-well plates. Both assays showed similar EC_{50} values in the presence of a PDE inhibitor, a requirement given for the TRF assay (Figure 3, panel c). Using 22F in the absence of a PDE inhibitor revealed a 10-fold increase in the EC_{50}, indicating the artificial bias that PDE inhibitors can have on compound pharmacology. Assay sensitivity (S/N) was greater for 22F at all doses (Figure 3, panel d), in either the presence or absence of a PDE inhibitor. At saturating doses of PGE2, the assay window for 22F was 29-fold greater than TRF (S/N ratio of 230 versus 8). Similar results were seen when performing the comparison using the highest affinity antibody conjugate available for the TRF assay and fewer cells per sample (Supplementary Figure 7). Comparable results were also seen when assaying Gi-coupled receptors, where we noted similar or significantly improved Z′ values[10] at saturation for 22F (Supplementary Figures 8−10). Importantly, the sensitivity of 22F can allow assays of Gi-coupled receptors to be conducted in the absence of added forskolin. Recently, use of the 20F construct has been validated in HTS format, where the live-cell, nondestructive nature of the assay was found to be well suited for screens of allosteric modulators of GPCR function.[9]

We have developed a real-time biosensor assay that allows the sensitive and accurate detection of GPCR mediated signaling through the second messenger cAMP. In contrast to lytic assays with multiple samples and procedural steps, cAMP dynamics can be followed from a population of living cells with greatly reduced time and labor. When compared to existing biosensor designs, our evolved biosensor construct provides a greatly increased dynamic range, making it better suited to monitor a broad range of receptor behaviors such as treatment with full, partial, or inverse agonists (Supplementary Figure 11).[11] The combined characteristics of real-time kinetics, enhanced sensitivity, and broad dynamic range provide an assay that is well suited to monitor the complex biology surrounding cellular cAMP, including physiologically important events such as receptor desensitization and cAMP turnover (Supplementary Figure 12).[1,9] The live cell, nondestructive format affords opportunities to multiplex assays in the study of biased agonism,[2,12,13] together with providing novel screening formats to identify allosteric modulators of GPCR function.[9] Such characteristics are expected to facilitate both drug discovery and academic research efforts.

dx.doi.org/10.1021/cb200248h |*ACS Chem. Biol.* 2011, 6, 1193–1197

METHODS

Unless otherwise specified, catalog numbers refer to products available from Promega Corporation.

Directed Evolution. *Constructs.* All biosensor variants were constructed in either the vector pF1K (Promega) or a modified version of pF9A (Promega) containing an *E. coli* ribosome binding site.

Assays. Mutants/libraries were generally overexpressed in KRX *E. coli* and screened as bacterial lysates in 96-well microtiter plates for increased luminescence in response to exogenously added cAMP (50 uM), and then variants of interest were further screened as transient transfections in HEK-293 cells for response to 10 μM isoproterenol (agonist of endogenous B2-adrenergic receptor). In some cases variants were screened directly in HEK-293 cells.

Rational design of cAMP binding domain. To engineer variants with altered binding affinity for cAMP we used an alignment of 38 eukaryotic PKA-R sequences from SwissProt to identify positions where a particular amino acid was present in at least 45% of the aligned sequences (Cochran *et al.*, 2006). If the biosensor RIIβB residue at each of these positions did not match the most frequent amino acid, then it was altered to that residue. Thirty-one variants were built by site-directed mutagenesis (Quickchange, Stratagene) and screened using both the bacterial and HEK-293 assays.

Linker mutagenesis. A library of 13,000 linker sequences connecting the N-terminal luciferase fragment to the cAMP binding domain was created and introduced to the biosensor by cassette mutagenesis where 10 (see underscored) of the 12 parental linker residues (GSSGGSGGSGGG) were randomized to the extent that each variant contained on average four random amino acid changes; 7,000 individual variants were screened using the bacterial assay, and 58 hits were then screened using the HEK-293 assay to determine which variant was the most improved.

Global random mutagenesis and combinatorial analysis. Using the entire biosensor sequence as template, an error-prone PCR (GeneMorph, Stratagene) library was created that contained on average 1−2 amino acid changes per clone; 9,000 individual variants were screened using the bacterial assay, and 94 hits were then screened using the HEK-293 assay to determine which variants were the most improved. Combination sequences consisting of the most beneficial mutations were constructed using site-directed mutagenesis and screened using the HEK-293 assay to determine the best combination sequence.

Biosensor Characterization *in Vitro*. The TNT T7 Coupled Reticulocyte Lysate System (cat. no. L4610) was used to express the biosensor variants encoded by the pGloSensor-20F cAMP (Genbank EU770615) and pGloSensor-22F cAMP plasmids (Genbank GU174434) following the listed protocol. Following expression, aliquots of lysate were combined with varying concentrations of cAMP (cat. no. V6421 serially diluted in dH_20) and incubated for 15 min at RT. Five microliters of lysate was combined with 100 μL of Luciferase Assay Reagent (cat. no. E1500) using reagent injectors, and luminescence was measured immediately on a GloMax luminometer (0.5 s integration time). Data plotted in Figure 2c and d represent the average of three separate measurements per dose, and the error is represented as the standard deviation. EC_{50} values were calculated using the four parameter logistic equation *via* Graph Pad Prism 4.

22F *vs* 20F Comparison in HEK293. *Day 1.* Cell plating and transient transfection. Exponentially growing HEK293 cells (T75 flask) were washed with DPBS (Invitrogen cat. no. 14190), treated with 0.05% trypsin-EDTA (Invitrogen cat. no. 25300), and resuspended to 3.21×10^5 cells/mL in DMEM (Invitrogen cat. no. 11995) + 10% FBS (Invitrogen cat. no. 16000) + 1x NEAA (Invitrogen cat. no. 11140). pGloSensor-22F cAMP (cat. no. E2301; 7 μg) or pGloSensor-20F cAMP (cat. no.E1171; 7 μg) plasmid DNA were combined with 700 μL of Opti-Mem I (Invitrogen cat. no. 31985) and combined with 21 μL of FuGENE HD (cat. no. E2311) for 10 min at RT. Cell suspension and lipid/DNA mixture were combined 20:1, and 100 μL per well was transferred to a 96-well plate (Corning cat. no. 3917) with incubation at 37 °C for 24 h.

Day 2. Existing medium was replaced with CO_2 independent medium (Invitrogen cat. no. 18045) + 10% FBS, and GloSensor cAMP Reagent (cat. no. E1290) was added to a 2% v/v final dilution from a 50x stock in 10 mM HEPES, pH = 7.5. Following incubation for 2 h at RT, preread measurements were acquired on a Varioskan Flash instrument (Thermo Electron; 0.1 s integration time) at 28 °C prior to compound addition. Following acquisition of a stable signal, varying concentrations of isoproterenol (ISO; Sigma cat. no. I5627), salbutamol (SALB; Sigma cat. no. S8260), salmeterol (SALM; Sigma cat. no. S2692), or forskolin (FSK; Sigma cat. no. F3917) plus 3-isobutyl-1-methylxanthine (IBMX; Sigma cat. no. I7018) were added from 10x stocks in CO_2 independent medium (serum-free), and luminescence was monitored continuously at 28 °C (the steady-state operating temperature of the instrument in kinetic mode; 0.2% v/v DMSO final in all wells). The luminescence of a given well post compound addition was divided by the final preread measurement of the same well to calculate fold response.

Comparison to Immunoassay. *Day 1.* Cell plating. HEK293 cells (15,000 cells/well; 100 μL) were plated to the individual wells of a 96-well plate (Corning cat. no. 3917) in DMEM + 10% FBS (Hyclone cat. no. SH30071) and grown overnight at 37 °C in 5% CO_2.

Day 2. Transient transfection (per well): pGloSensor-22F cAMP (cat. no. E2301; 100 ng) or pGloSensor-20F cAMP (cat. no. E1171; 100 ng) plasmid DNA was combined with 0.3 μL of TransIT-LT1 reagent (Mirus Bio; cat. no. MIR 2300) in 10 μL of CO_2 independent medium. After a 10 min incubation, 10 μL of lipid/DNA mixture was added per well, followed by incubation at 37 °C in 5% CO_2 for 20 h.

Day 3. Biosensor assay. Existing medium was replaced with CO_2 independent medium + 10% FBS, and GloSensor cAMP Reagent (cat. no. E1290) was added to a 2% v/v final dilution from a 50x stock in 10 mM HEPES, pH = 7.5. Following incubation for 1.5 h at RT, plates for the biosensor assay were read in a Varioskan Flash instrument (Thermo Electron; 0.5 s integration time) at 28 °C prior compound addition. Following acquisition of a stable signal, isoproterenol (1 μM; Sigma cat. no. I5627), propranolol (10 μM; Sigma cat. no. P0884), and forskolin (10 μM; Sigma cat. no. F3917) were added sequentially at the indicated time points (1 μL/well), and luminescence was monitored continuously. Alternatively, 100 nM isoproterenol (20 μL/well) alone was added, and luminescence was monitored continuously. Data plotted are the average of three separate wells; the error is represented as the standard deviation. *Immunoassay*. Existing medium was replaced with CO_2 independent medium +10% FBS and cells were incubated at RT for 1.5 h. Cells were then equilibrated in a 28 °C water bath, and isoproterenol, propranolol, and forskolin were added sequentially as described above. Alternatively, cells were treated with 100 nM isoproterenol alone. For each time point, medium was removed, 100 μL of 0.1 N HCl was added to the respective wells to promote cell lysis, and samples were subsequently frozen. All samples were later thawed and processed using the listed protocol (Assay Designs cat. no. 901−066, acetylated). Samples were diluted using 0.1N HCl for concentrations above 20 nM to be within the dynamic range of the standard curve. Data from individual wells were transformed *via* the curve fit of the cAMP standard curve (four parameter logistic curve fit; GraphPad Prism 4), where the values from three separate wells were then averaged to give the response at a given time point (error represented as the standard deviation). Alternatively, data were plotted as a percentage of the maximal response following addition of 100 nM isoproterenol.

Comparison to TRF Immunoassay. *Day 1.* HEK293 cells were seeded in DMEM + 10% FBS and grown overnight at 37 °C in 5% CO_2 (1.5×10^6 cells seeded in T75 flasks).

Day 2. pGloSensor-22F cAMP plasmid (cat. no. E2301) was diluted using Opti-MEM I to 12.5 ng/μL; 640 μL of diluted plasmid was combined with 24 μL of FuGENE HD (cat. no. E2311) and incubated at RT for 10 min. Existing medium in T75 flask was replaced with 8.3 mL of DMEM + 10% FBS + 664 μL of lipid/DNA mixture and incubated at 37 °C in 5% CO_2 for 22 h.

Day 3. Cells were dislodged *via* treatment with trypsin, pelleted, and resuspended in CO_2 independent medium (Invitrogen cat. no. 18045) + 10% FBS to 3×10^6 cells/mL. *Biosensor assay.* Cells were diluted further to 1.5×10^6 cells/mL using CO_2 independent medium + 10% FBS, and the GloSensor cAMP Reagent (cat. no. E1290) was added to a 2% v/v final dilution from a 50x stock in 10 mM HEPES, pH = 7.5. Following equilibration with substrate for 1.5 h at RT, 10 μL of cell suspension was transferred per well to a low volume 384-well plate (Corning cat. no. 3673), and 10 μL of PGE2 agonist was added from respective 2x stock solutions (see below). Luminescence was measured after a 30 min incubation with varying concentrations of PGE2 agonist (100 ms integration time; Varioskan Flash). *TRF immunoassay* (Cis-Bio Bioassays cat. no. 62AM6PEB). A 5 μL sample of the 3×10^6 cells/mL suspension was transferred to the individual wells of a low volume 384-well plate, and 5 μL of 2x PGE2 stocks was added to respective wells and incubated at RT for 30 min. Next 5 μL of d2-cAMP was added , followed by addition of 5 μL of anti-cAMP cryptate antibody. After a 1 h incubation at RT, time-resolved fluorescence was measured on a BMG Pherastar instrument [HTRF optic module; 10.1 mm focal height; 0.1 s positioning delay; 100 flashes per well; integration start at 60 μs; 400 μs integration time; simultaneous dual emission]. *PGE2 stocks.* 100x stocks of PGE2 agonist (Sigma cat. no. P5640) in DMSO. 50x dilution using CO_2 independent medium (serum-free) ± 200 μM IBMX (from 100 mM IBMX stock solution in DMSO).

■ ASSOCIATED CONTENT

Supporting Information. This material is available free of charge *via* the Internet at http://pubs.acs.org.

■ AUTHOR INFORMATION

Corresponding Author

*E-mail: brock.binkowski@promega.com.

Notes

The authors declare competing financial interests.

■ ABBREVIATIONS

cAMP: cyclic adenosine monophosphate; GPCR: G-protein coupled receptor; PKA: protein kinase A; HTS: high-throughput screening; RIIβB: B cAMP binding domain from PKA regulatory subunit type IIβ; S/B: signal/background; S/N: signal/noise; EIA: enzyme linked immunoassay; TRF: time-resolved fluorescence; PDE: phosphodiesterase

■ REFERENCES

(1) Violin, J. D., DiPilato, L. M., Yildirim, N., Elston, T. C., Zhang, J., and Lefkowitz, R. J. (2008) Beta2-adrenergic receptor signaling and desensitization elucidated by quantitative modeling of real time cAMP dynamics. *J. Biol. Chem. 283*, 2949–2961.

(2) Rajagopal, S., Rajagopal, K., and Lefkowitz, R. J. (2010) Teaching old receptors new tricks: biasing seven-transmembrane receptors. *Nat. Rev. Drug Discovery 9*, 373–386.

(3) McDonald, P. H., and Lefkowitz, R. J. (2001) [beta]Arrestins: New roles in regulating heptahelical receptors' functions. *Cell. Signalling 13*, 683–689.

(4) Hill, S. J., Williams, C., and May, L. T. (2010) Insights into GPCR pharmacology from the measurement of changes in intracellular cyclic AMP; advantages and pitfalls of differing methodologies. *Br. J. Pharmacol. 161*, 1266–1275.

(5) Willoughby, D., and Cooper, D. M. F. (2008) Live-cell imaging of cAMP dynamics. *Nat. Methods 5*, 29–36.

(6) Jiang, L. I., Collins, J., Davis, R., Lin, K.-M., DeCamp, D., Roach, T., Hsueh, R., Rebres, R. A., Ross, E. M., Taussig, R., Fraser, I., and Sternweis, P. C. (2007) Use of a cAMP BRET sensor to characterize a novel regulation of cAMP by the sphingosine 1-phosphate/G13 pathway. *J. Biol. Chem. 282*, 10576–10584.

(7) Fan, F., Binkowski, B. F., Butler, B. L., Stecha, P. F., Lewis, M. K., and Wood, K. V. (2008) Novel genetically encoded biosensors using firefly luciferase. *ACS Chem. Biol. 3*, 346–351.

(8) Binkowski, B., Fan, F., and Wood, K. (2009) Engineered luciferases for molecular sensing in living cells. *Curr. Opin. Biotechnol. 20*, 14–18.

(9) Pantel, J., Williams, S. Y., Mi, D., Sebag, J., Corbin, J. D., Weaver, C. D., and Cone, R. D. (2011) Development of a high throughput screen for allosteric modulators of melanocortin-4 receptor signaling using a real time cAMP assay. *Eur. J. Pharmacol. 660*, 139–147.

(10) Zhang, J. H., Chung, T. D., and Oldenburg, K. R. (1999) A simple statistical parameter for use in evaluation and validation of high throughput screening assays. *J. Biomol. Screening 4*, 67–73.

(11) Wisler, J. W., DeWire, S. M., Whalen, E. J., Violin, J. D., Drake, M. T., Ahn, S., Shenoy, S. K., and Lefkowitz, R. J. (2007) A unique mechanism of beta-blocker action: Carvedilol stimulates beta-arrestin signaling. *Proc. Natl. Acad. Sci. U.S.A. 104*, 16657–16662.

(12) Robers, M., Stecha, P., Karassina, N., Binkowski, B., Fan, F., Cong, M. (2011) Multiplexed Analysis of Second Messenger Signaling in Live Cells Using Aequorin and GloSensor cAMP on the Hamamatsu uCell., p SBS 17th Annual Conference and Exhibition, Orlando, FL.

(13) Luttrell, L. M., and Gesty-Palmer, D. (2010) Beyond desensitization: Physiological relevance of arrestin-dependent signaling. *Pharmacol. Rev. 62*, 305–330.